Original Article

Comparison and Validation of Multiple Detectors against Monte Carlo Simulation for the Use of Small-Field Dosimetry

Nazia Parveen, Prabhakar Ramachandran, Venkatakrishnan Seshadri, Ben Perrett, Andrew Fielding[1]

Therapeutic Physics, Radiation Oncology, Cancer Services, Princess Alexandra Hospital, Woolloongabba, Queensland, [1]School of Chemistry and Physics, Queensland University of Technology (QUT), Brisbane, Australia

Abstract

Aim: The aim of this study was to compare the Exradin W2 scintillator, PTW microDiamond, IBA Razor Nano, and IBA Razor chamber detectors for small-field dose measurements and validate the measured data against the EGSnrc user code and observe the variation between daisy-chained and direct measurement methods for the above detectors. **Materials and Methods:** The W2 scintillator, microDiamond, Razor Nano, and Razor chamber detectors were used to measure the in-plane and cross-plane profiles and the output factors (OFs) at 10 cm depth, and 90 source-to-surface distance for 6MV X-rays (Elekta Versa HD). The field sizes ranged from 0.5 cm × 0.5 cm to 5 cm × 5 cm. The BEAMnrc/DOSXYZnrc user codes (EGSnrc) were used to simulate the reference profiles. Gamma analysis was performed to compare the measured and simulated dose distributions. **Results:** The OFs measured with the W2 scintillator, microDiamond, Razor Nano chamber, Razor chamber, and the calculated Monte Carlo (MC) showed agreement to within 1% for the 3 cm × 3 cm field size. The uncertainty in the MC simulation was observed to be 0.4%. The percent difference in OFs measured using daisy-chained and direct measurement methods was within 0.15%, 0.4%, 1.4%, and 2.4% for microDiamond, W2 scintillator, Nano, and Razor chamber detectors, respectively. **Conclusion:** The lateral beam profiles and OFs of W2 scintillator, microDiamond, Razor Nano, and Razor chambers exhibit good agreement with the MC simulation within the nominal field sizes. Our results demonstrate that we can achieve considerable time-saving by directly measuring small-field OFs without daisy-chained methods using microDiamond and W2 scintillator. In terms of ease of use, sensitivity, reproducibility, and from a practical standpoint, we recommend microDiamond for small-field dosimetry.

Keywords: Monte Carlo simulation, radiation detectors, small-field dosimetry

Received on: 05-05-2022 **Review completed on: 30-06-2022** **Accepted on: 20-07-2022** **Published on: 08-11-2022**

Introduction

Techniques such as intensity-modulated radiation therapy, volumetric-modulated radiation therapy, stereotactic body radiation therapy, Gamma Knife, and CyberKnife often deliver dose distributions to small targets while employing steep dose gradients.[1] These techniques increasingly use small-field sizes, and hence, small-field dosimetry methodology is necessary for accurate commissioning and validation of treatment planning for these techniques.

Conventional radiotherapy is based on the commonly used code of practices (COPs) published by the International Atomic Energy Agency (IAEA) TRS-398[2] and the American Association of Physicists in Medicine (AAPM) TG-51 protocols.[3] These protocols are designed for reference dosimetry in conventional field sizes, typically 10 cm × 10 cm, and employ ionization chamber measurements to find the absorbed dose to water under reference conditions. Reference fields smaller than this are not addressed in these COPs. To address the reference dosimetry of small fields used in external beam therapy, the IAEA in collaboration with the AAPM introduced the first code of practice for small-field dosimetry, TRS-483, which provides a protocol for measurements of small-field profiles and output factors (OFs)[4] in external beam radiotherapy.

Access this article online

Quick Response Code:

Website: www.jmp.org.in

DOI: 10.4103/jmp.jmp_35_22

Address for correspondence: Dr. Prabhakar Ramachandran, Cancer Services, Princess Alexandra Hospital, Woolloongabba, Queensland 4102, Australia. E-mail: prabhakar.ramachandran@health.qld.gov.au

How to cite this article: Parveen N, Ramachandran P, Seshadri V, Perrett B, Fielding A. Comparison and validation of multiple detectors against monte carlo simulation for the use of small-field dosimetry. J Med Phys 2022;47:235-42.

Small fields with radiation portals smaller than the range of secondary electrons in a medium typically exhibit loss of lateral charged particle equilibrium. In addition, the finite-sized radiation source may be partially occluded by the collimator system, introducing changes in the beam profile and spectrum. The characteristics of a radiation detector, such as size, shape, and material, play an essential role in its response to ionizing radiation. In addition, the response of a detector can vary considerably with radiation field size. If the active volume of a detector is large relative to the field size, then a significant volume averaging effect will occur. The density of the detector's active volume and the material(s) that make up the detector can also influence the detector response in small fields. Therefore, selecting a suitable detector for small-field dosimetry is crucial for accurate dose measurement. A detector with high spatial resolution, low noise, water equivalence, low directional, and energy dependence is considered ideal, but no detector has all these properties.[5] Many studies have been published using different types of detectors. Stasi *et al*. studied the performance of several micro-ionization chambers in small fields.[6] The OFs of all the chambers in their study were compared to that of the microDiamond detector, where all the detectors showed a good agreement of within 2% to the microDiamond detector for field sizes greater than1 cm × 1 cm while the Exradin A16 micro-ionization chamber had even closer agreement at 1 cm × 1 cm.

Scintillation material has been in use to detect radiation for a very long time.[7] Scintillators work on the principle of emission of visible light upon excitation by ionizing radiation. An ideal scintillator should convert a large fraction of the incident radiation to visible light and at the same time minimize the undesirable phosphorescence and delayed fluorescence. The prompt emission of visible light is responsible for the signal used for dose measurement.[8]

One limitation observed in scintillators is Cerenkov light emission, which generates a superfluous signal alongside the scintillator light and is produced when electrons move faster than light in the material.[9] The amount of Cerenkov light is proportional to the length of the fiber exposed to radiation. This problem can be reduced by using different approaches such as the spectral method, which uses the ratio of the signal in two spectral regions delivered in different detector arrangements (to minimize and maximize Cerenkov light) to correct for the Cerenkov signal.[10] A recent application of the spectral method is found in a commercially available plastic scintillator, the Exradin W1, which has a dimension of 1 mm diameter × 3 mm length. A comprehensive study of the characteristics of the Exradin W1 scintillator illustrates it as an excellent alternative to other detectors used in small fields.[11]

A relatively new detector called the Exradin W2 scintillator has an improved measurement resolution for small-field dose measurements because of its small size, i.e., 1 mm × 1 mm and 1 mm × 3 mm sizes available. The W2 electrometer can be connected to other measurement systems, allowing scanning of small-field profiles and PDDs in real time. In a recent study, the W2 in small fields has been compared to GAFChromic EBT-3 film and the W1 scintillator. The PDD measurements and OFs were also compared to the W1 scintillator detector, while dose profiles were compared to GAFChromic EBT-3 film. Other parameters investigated included dose rate linearity and temperature dependence. The study showed that the W2 scintillator detector has a similar response as the W1 scintillator, with the only difference being its capability of beam scanning, making it an ideal detector for small fields.[12]

The IBA Razor Nano chamber is the smallest ionization chamber currently available, with a cavity volume of 0.003 cm^3. This chamber's active volume and electrodes are designed to be similar to concentric spheres, reducing directional dependence. The properties of the IBA Razor Nano chamber have been investigated in small fields and have been proved to be suitable for dose profile measurements in field sizes down to 2 cm × 2 cm.[13] microDiamond detectors have been considered a good choice for small-field dosimetry due to high spatial resolution, tissue equivalence, high sensitivity, small size, low leakage current, and limited directional dependence.[14] A thorough review of commercial and prototype microDiamond detectors, their performance in megavoltage photon beams, and factors affecting their dosimetric properties are presented by Talamonti *et al*.[15]

This study is designed to evaluate and verify the properties of the W2 scintillator detector, microDiamond detector, Razor Nano chamber, and Razor chamber detector in small fields compared to Monte Carlo (MC) simulations. The beam profile and OFs have been investigated in field sizes from 0.5 cm × 0.5 cm up to 3 cm × 3 cm for an Elekta Versa HD™ linear accelerator.

Materials and Methods

Monte Carlo simulations

The BEAMnrc and DOSXYZnrc user codes of the EGSnrc software toolkit (EGSnrc v2019) were used for all MC simulations.[16,17] An Elekta Versa HD LINAC with agility multileaf collimator (MLC) was modeled for a 6 MV photon beam using the BEAMnrc user code. The parameters for the MC simulation were taken from Elekta technical documentation, with minor changes made to improve the matching between measured and simulated data. The most notable change in the parameters is the introduction of a small rotation of about –0.004 radians of the agility MLC bank to best approximate the divergent leaf design employed by the Elekta Versa HD to reduce interleaf leakage. The optimal leaf bank rotation (LBROT) angle was selected by comparing simulated and measured dose profiles by varying LBROT angle for a 2 cm × 2 cm field size until the best agreement was found. For each simulation, fifty billion histories were used for simulation with a statistical uncertainty of 0.4% estimated by batch method.

The MLCE component module in BEAMnrc was used for modeling the agility MLC wherein all leaves are identical and can be tilted about an axis that runs parallel to the opening direction of the leaves. The whole leaf bank can be rotated by a user-specified angle to increase focus. The MLCQ component module was used to model the lower jaws. This component module models MLCs or jaws with rounded leaf/jaw ends, with the radius of the jaw ends and Z position specified by the user for focusing. The number of agility MLC leaf pairs used was 80 (a total of 160 MLC leaves), with cylindrical leaf ends using a radius of curvature of 17 cm and 0.5 cm wide at the isocenter. An in-house spreadsheet was used to calculate the MLC and jaw positions for square fields. The MLC leaves were modeled parallel to the y-axis and jaws parallel to the x-axis. A geometrical illustration of the different component modules, their arrangement, and composition is shown in Figure 1.

Configurations with nominal square field sides 0.5 cm, 0.6 cm, 0.7 cm, 0.8 cm, 1.0 cm, 2.0 cm, 3.0 cm, 4.0 cm, 5.0 cm, and 10.0 cm were modeled. An elliptical beam source with a Gaussian distribution (source number 19 in BEAMnrc) was used to model the electron beam incident on the target. The electron beam size was taken as 0.20 cm in the x-direction and 0.28 cm in the y-direction with an electron beam energy on the bremsstrahlung target of 6.5 MeV. All simulations were run for 50 million histories with the photon cutoff energy and electron cutoff energy set to 0.01 MeV and 0.7 MeV, respectively. In this study, photon forcing variance reduction techniques was used to increasing the efficiency of MC simulation. An annular dose scoring plane was selected after the last component module (slab), and all other transport parameters were set to default. The materials as defined in the pegs4dat file were taken from Elekta's technical documentation. The maximum CPU hours was set to 1000 h, and for a typical simulation, the run time was between 48 and 60 h. The transport parameters were set to default values. These simulations generated phase-space files that were used for simulating the absorbed dose to a water phantom at 90 cm source-to-surface distance (SSD). The BEAMnrc model was validated against the measured PDDs and lateral profiles for a field size of 10 × 10 cm^2 at 10 cm depth.

The water phantom size was defined in DOSXYZnrc as per the field size. For a 1 cm × 1 cm field size, the size of the water phantom was 4.05 cm × 4.05 cm × 12.5 cm, corresponding to 81 × 81 × 250 voxels. The size of each voxel was 0.05 cm × 0.05 cm × 0.05 cm. The number of voxels in the x and y direction was increased by 10 voxels with the increasing field size for the other field sizes. The reason for changing the size of the phantom in the x–y direction was to account for scatter contribution for larger fields. The medium of the phantom was selected as water, and its surrounding layer was set to air.

The phase-space file scored at the last component module in the BEAMnrc simulation was used as a source in DOSXYZnrc. Theta was set to 180° to simulate the gantry at 0° and all other angles and coordinates of the isocenter were set to zero. The job was then submitted in ten batches and simulations run using a high-performance SGI Altix XE Linux cluster with 212 computer nodes. The 3ddose files were converted into dose reading using a script written in MATLAB. The OFs were calculated at the central axis at 10 cm depth with each field normalized to the central voxel at 10 cm depth of the reference field (4 cm × 4 cm and 10 cm × 10 cm).

Small-field measurements

Measurements were performed using an Exradin W2 plastic scintillator detector, IBA Razor Nano chamber, IBA Razor

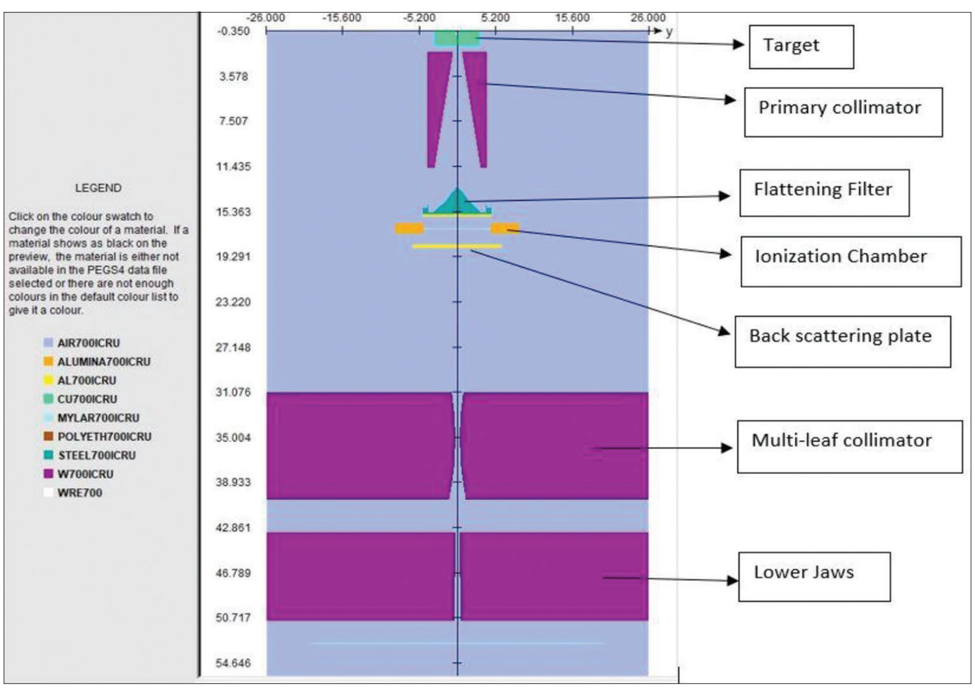

Figure 1: A geometrical illustration of the component modules of the accelerator used in the BEAMnrc

chamber small volume ionization chamber, and a PTW microDiamond detector. Specifications for the detectors can be found in Table 1. The W2 scintillator detector comes with a MAX SD electrometer designed to process the signal with a built-in Cerenkov correction feature.

A Blue Phantom 2 scanning water tank was used for all measurements. IBA OmniPro-Accept 7.4 software was used to set the scanning input parameters and to acquire and process the data. The step-by-step mode was used for profile scans to improve accuracy, and profiles were delivered using a step size of 1 mm and measurement time of 1 s per dwell position for field sizes <1 cm × 1 cm. For field sizes >1 cm × 1 cm, continuous scans were performed at the speed of 3 mm/s. An IBA Stealth Chamber was present for all measurements and used as a reference detector. The inline and crossline profiles were measured in an IBA Blue Phantom 2 at 10 cm depth with a stealth detector used as reference. An inline profile was first measured at 90 cm SSD and 10 cm depth to determine the deviation in the central axis. The chamber position was corrected to the centre of the field, and the scan was repeated for confirmation. The same procedure was repeated for crossline direction. To determine the perpendicularity of inline and crossline scan planes to beam central axis, profiles were obtained at 5 cm, 15 cm, and 20 cm depth to ensure the central axis deviations for these scans to be <0.1 mm.

For OFs, the W2-1 × 1 scintillator detector, microDiamond detector, Razor Nano chamber, and Razor chamber were connected to the PTW UNIDOS electrometer to measure OFs at 10 cm depth for each field size with a delivery of 100 MU per reading. Reference conditions for OF measurement were 90 cm SSD at 10 cm depth in water compared to a reading for a 10 cm × 10 cm field. Following the recommendations of TRS-483 and the vendors, the Razor Nano, Razor chamber, microDiamond, and W2-1 × 1 scintillator were mounted in the vertical orientation (aligned parallel to the beam central axis). Profiles and OFs were measured for 6 MV beams at nominal field sides of 0.5 cm, 0.6 cm, 0.7 cm, 0.8 cm, 1.0 cm, 2.0 cm, 3.0 cm, 4.0 cm, 5.0 cm, and 10.0 cm. The detector was aligned with the center of the profiles prior to OF measurement using the determined position of the center of the beam profiles using IBA Omnipro-Accept. Measurements were performed until the output stabilized, and were corrected for the influence of temperature and pressure. Final OFs were determined as recommended by TRS-483 by using an IBA CC13 chamber to measure OFs for an intermediate reference field of 4 cm × 4 cm.

Analysis

An in-house software written in MATLAB™ was used for performing the gamma analysis to assess the similarity of measured and simulated dose profiles.[18] A linear interpolation of the measured data was used to create a reference dataset with a spatial resolution of 0.1 mm to reduce the artificial increase in the distance-to-agreement between two data pairs due to the discrete nature of the data. The datasets for each field size and direction were manually aligned and normalized to 100% at the maximum dose. The gamma analysis was normalized to the maximum dose and was performed above a dose threshold of 10% within specified nominal field size. To reduce the noise in the MC profiles, a median filter was used in MATLAB with window length specified to 7 mm. The uncertainty in the MC simulation was observed to be 0.4%. Statistical analyses were performed using R-Software.

Results

The corresponding measured and simulated profiles plotted together are given in Figures 2-5. The x-axis represents the off-axis distance in cm and y-axis indicates the dose normalized to 100%. A comparison of the profiles clearly displays areas of agreement and differences. These profiles represent the dose distribution along the in-plane and cross-plane at 10 cm depth in a water phantom.

Figures 2-5 represent the cross-plane and in-plane lateral beam profiles of all the detectors compared to the MC simulated for field sides of 0.5 cm, 0.6 cm, 0.7 cm, 0.8 cm, and 3.0 cm.

The results of the gamma analysis for the in-plane and cross-plane profiles for all the detectors show a passing rate of above 90% for gamma criteria 3%/2 mm for all the detectors at different field sizes, as shown in Table 2.

Table 1: Specification of the detectors used in this paper

Detector	Dimensions of active volume	Material	Shape of active volume
W2 scintillator	Diameter: 1 mm Length: 1 mm Volume: 0.8 mm^3	Polystyrene with ABS plastic enclosure and polyimide stem Acrylic with polyethylene jacket	Cylindrical
Razor Nano	Diameter: 2 mm Volume: 3 mm^3	Central electrode: Graphite Wall: Shonka C552	Spherical
Razor chamber	Diameter: 2 mm Length: 3.6 mm Volume: 10 mm^3	Central electrode: Steel Wall: Shonka C552	Cylindrical
microDiamond	Volume: 0.004 mm^3 Radius: 1.1 mm Thickness: 1 µm	Synthetic single crystal microDiamond	Disk

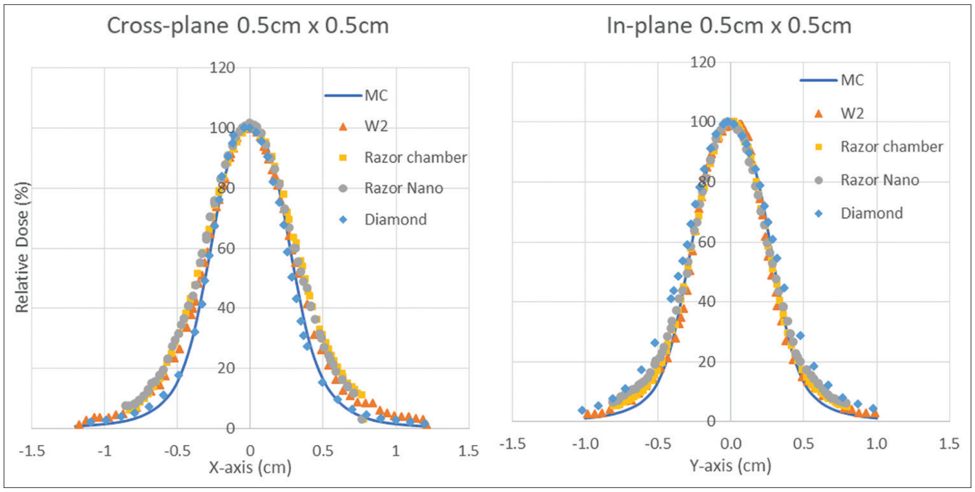

Figure 2: Cross-plane and in-plane profile of a 0.5 cm × 0.5 cm field at 10 cm depth of W2 scintillator, normalized, Razor Nano, and Razor chamber compared to the Monte Carlo profile

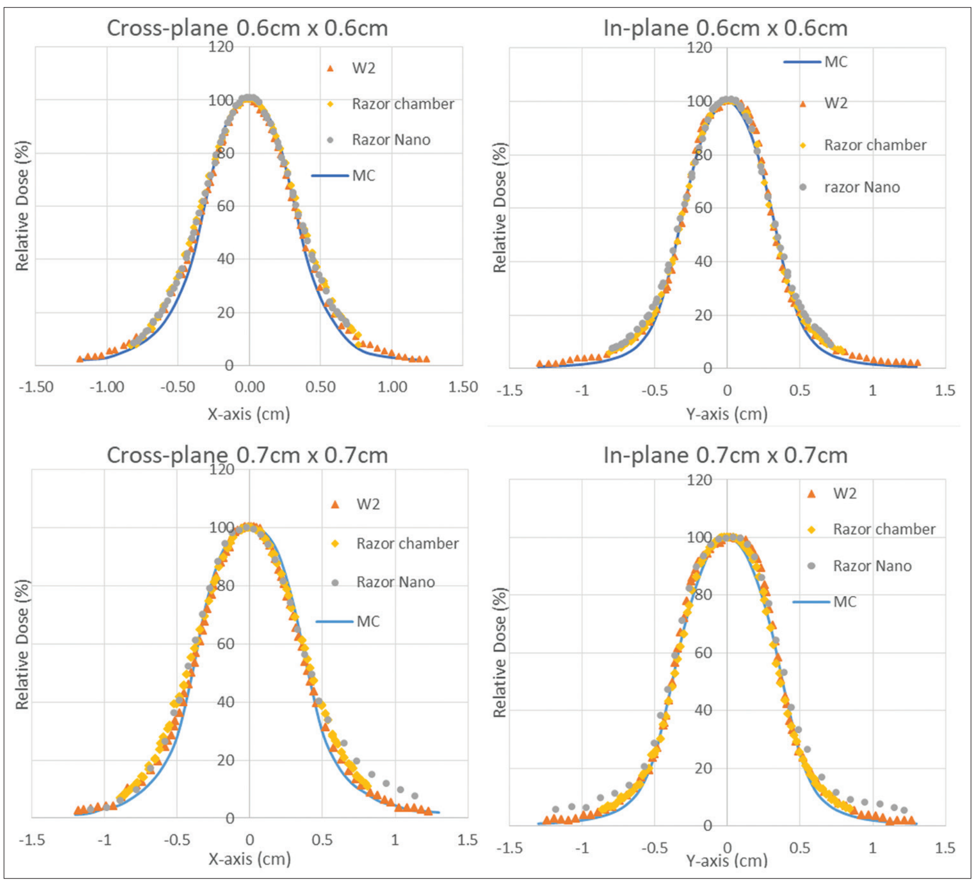

Figure 3: Cross-plane and in-plane profile of a 0.6 cm × 0.6 cm (top) and 0.7 cm × 0.7 cm field (bottom) at 10 cm depth of W2 scintillator, normalized, Razor chamber, Razor Nano, and MC. MC: Monte Carlo

Output factors

Figure 6 plots output factors against measured field size without the use of an intermediate reference field. The results demonstrate that the microDiamond gives equivalent output factors without the use of a reference field. The measured OFs daisy-chained to an intermediate 4 cm × 4 cm field were plotted against the measured field size and compared to the calculated OF, as shown in Figure 7. It shows a good agreement between the OFs measured using W2 and microDiamond with the MC calculated OF, while the Razor chamber and Razor Nano show a deviation from the MC data as the field size decreases.

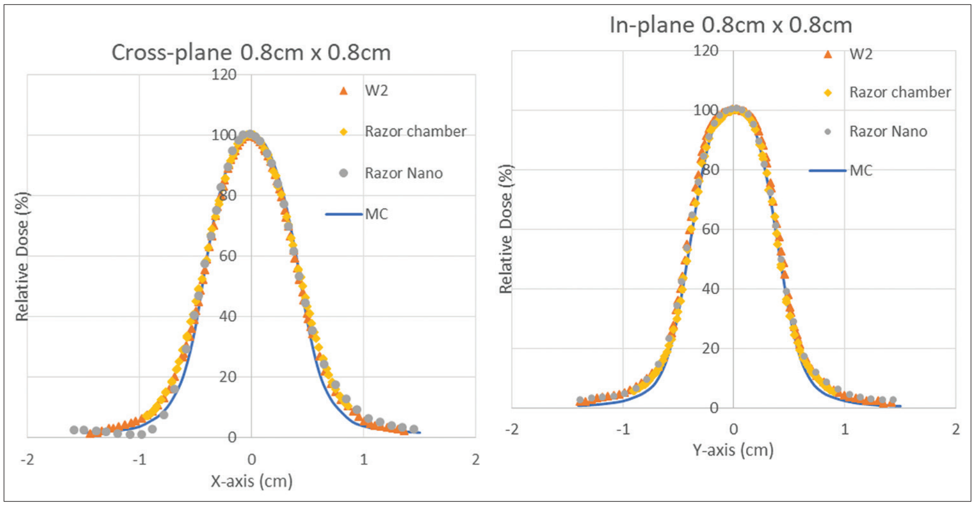

Figure 4: Crossline and inline profile of a 0.8 cm × 0.8 cm at 10 cm depth of W2 scintillator, Razor Nano, and Razor chamber detector compared to the Monte Carlo

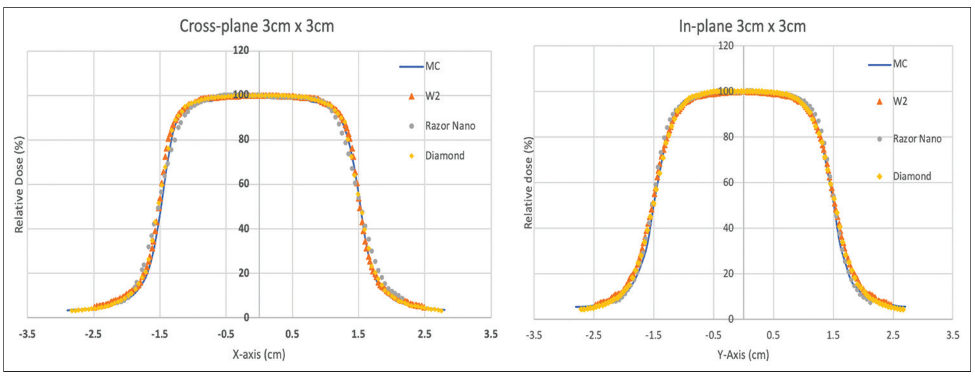

Figure 5: Cross-plane and in-plane profile of 3 cm × 3 cm field at 10 cm depth for different detectors compared against MC. MC: Monte Carlo

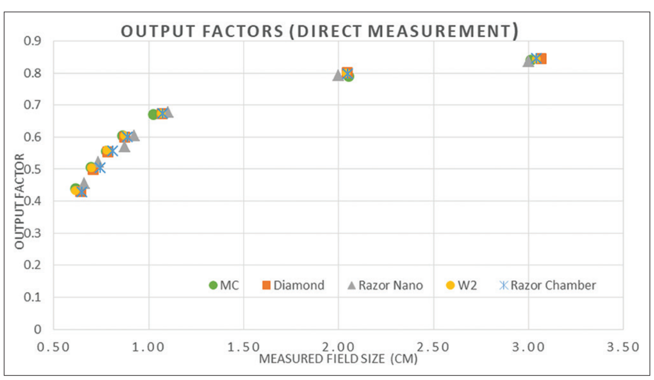

Figure 6: A graphical comparison of output factors of W2 scintillator, microDiamond detector, Razor Nano chamber, Razor chamber, and Monte Carlo data normalized to 10 cm × 10 cm

Discussion

In our study, the beam profiles and OFs measured using W2 scintillator detector, microDiamond detector, Razor Nano chamber, and Razor chamber detector were evaluated against MC-simulated data in small fields. Many studies have focused on comparing these detectors with other small-field detectors as well as an intercomparison of microDiamond across multiple centers.[12,19,20]

The beam profiles indicate acceptable performance for all detectors studied, with a small volume averaging effect visible for the Razor and Razor Nano chambers, causing a slight broadening of the small-field profiles. This is due to the large size of the active volume relative to the field size. Despite its small size, the W2 scintillator detector exhibited variation in the penumbral region of very small fields (0.5 cm, 0.6 cm, 0.7 cm, and 0.8 cm) compared to MC simulation. The agreement improves for field sizes >1 cm. Galavis *et al*. have studied the dosimetric properties of the W2 scintillator by comparing dose profiles of the W2 with that of a GAFChromic film and W1 scintillator where the dose difference was found to be within 0.5% for a 1 cm × 1 cm field.[12] Further analysis of the 1 cm × 1 cm field of W2 scintillator detector shows a passing rate of above 90% at 2%/2 mm gamma criteria compared to the MC data, which makes it a good alternative for the microDiamond for small-field dosimetry.

The microDiamond and W2 are close to an ideal water-equivalent detector for small-field measurements in a 6 MV beam. The W2

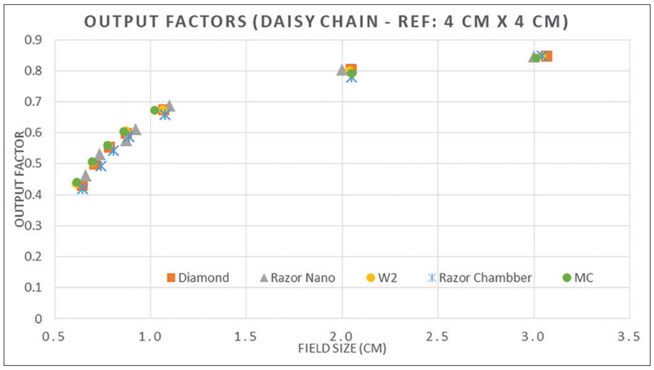

Figure 7: A graphical comparison of output factors of W2 scintillator, microDiamond detector, Razor Nano chamber, Razor chamber, and Monte Carlo data normalized to an intermediate field (4 cm × 4 cm)

scintillator can be used without field output correction factors for small fields,[4] but published field output correction factors for the microDiamond deliver equivalent OF measurements. The microDiamond generates a relatively strong signal, is easy to use directly with a water tank scanning system, and was found to give equivalent OF results without the use of an intermediate field, making it an excellent choice for small-field measurements where time is an issue. The dosimetric properties of synthetic single-crystal microDiamond detectors, such as the microDiamond, have previously been investigated by Ciancaglioni *et al*. by comparing the results with that obtained with PTW type 31014 PinPoint micro-ionization chamber and were found in good agreement.[21] We observed lateral beam profiles matched very closely (to within 1%) to the W2 scintillator detector throughout the investigated field size.

Results were consistent for in-plane and cross-plane profiles. Note that the cross-plane profiles are broader than the in-plane profiles for field size smaller than 1 cm which is caused by the relative position of the leaf bank and jaw in the treatment head.

The Razor Nano has a spherical geometry for the electrodes and active volume and is recommended to be mounted vertically (aligned with the beam axis) for beam profile and OF measurements by the manufacturer. The low signal to noise ratio due to small volume of the Razor Nano chamber poses a challenge when measuring profiles and generally requires long stabilization time. The OF of Razor Nano chamber normalized to the 4 cm × 4 cm reference field was found to be in good agreement (2%) with the other detectors in field size greater than 1 cm while the agreement decreases in smaller field size due to the effect of volume averaging. This agrees with the result obtain by Reggiori *et al*. for the Razor Nano chamber compared to Razor chamber and microDiamond detector.[19]

The OFs of the W2 scintillator and microDiamond show good agreement with MC calculated OFs for small fields. The percentage difference for the W2 scintillator and MC falls within 2% for all field sizes with a maximum percentage difference of 1.5% for 0.5 cm nominal field size. The OF measured with microDiamond had a maximum difference of 2.2% for 0.5 cm field when compared to the MC model.

Table 2: Gamma passing rates for the measured and Monte Carlo cross-plane and in-plane profiles at 3%/2 mm gamma criteria analyzed within the norminal field size

Detector type	Field size	Gamma criteria 3%/2mm	
		Cross-plane Pass rate (%)	In-plane Pass Rate (%)
W2 Scintillator detector	0.5	97	93
	0.6	100	95
	0.7	100	99
	8	99	97
	3	98	94
Razo chamber	0.5	98	94
	0.6	100	96
	0.7	99	97
	0.8	99	100
Razor nano	0.5	98	97
	0.6	100	99
	0.7	99	93
	0.8	99	93
	3	96	98
microDiamond	0.5	99	96
	1	98	96
	3	99	99

A publication by Monasor Denia *et al*. in 2019 contains OFs for microDiamond measured in a 6 MV beam under equivalent conditions to our measurements, with OFs of 0.518 for the 0.6 cm × 0.6 cm field and 0.794 for 1 cm × 1 cm field.[22] Our measurements are in agreement with these values. As per TRS-483, the Razor ionization chamber requires larger field output correction factors due to volume averaging as the detector is large relative to field size.

Conclusion

Beam profiles and OFs were successfully measured for the W2 scintillator, microDiamond, Razor Nano, and Razor chamber detectors and found to be in good agreement with MC simulations for equivalent field sizes. These results confirm that all detectors are suitable for small-field dosimetry in a 6 MV beam. In terms of ease of use, accuracy of measurement, and sensitivity, the microDiamond is an excellent choice. It should be noted that TRS-483 recommends the use of at least three different types of small-field detectors to characterize small fields.

Acknowledgments

The authors thank Drs Paul Charles, Scott Crowe and Thomas O'Brien for their support and comments.

Financial support and sponsorship

This study was partly supported by SERTA grant.

Conflicts of interest

There are no conflicts of interest.

References

1. Das IJ, Ding GX, Ahnesjö A. Small fields: Nonequilibrium radiation dosimetry. Med Phys 2008;35:206-15.
2. An International Code of Practice for Dosimetry Based on Absorbed Dose to Water IAEA Tech. Series No. 398, Absorbed Dose Determination in External Beam Radiotherapy. Vienna: IAEA; 2000.
3. Almond PR, Biggs PJ, Coursey BM, Hanson WF, Huq MS, Nath R, *et al.* AAPM's TG-51 protocol for clinical reference dosimetry of high-energy photon and electron beams. Med Phys 1999;26:1847-70.
4. International Atomic Energy Agency. Technical Reports Series no. 483; Dosimetry of Small Fields Used in External Beam Radiotherapy- An International Code of Practice for Reference and Relative Dose Determination. Vienna: IAEA; 2017.
5. Parwaie W, Refahi S, Ardekani MA, Farhood B. Different dosimeters/detectors used in small-field dosimetry: Pros and cons. J Med Signals Sens 2018;8:195-203.
6. Stasi M, Baiotto B, Barboni G, Scielzo G. The behavior of several microionization chambers in small intensity modulated radiotherapy fields. Med Phys 2004;31:2792-5.
7. Weber MJ. Inorganic scintillators: Today and tomorrow. J Luminescence 2002;100:35-45.
8. Knoll GF. Radiation detection and measurement. 3rd ed., Ch. 8. Hoboken, New Jersey, USA, John Wiley & Sons; 1999.
9. Beaulieu L, Goulet M, Archambault L, Beddar S. Current status of scintillation dosimetry for megavoltage beams. J Phys Conf Ser 2013;444:012013.
10. Guillot M, Gingras L, Archambault L, Beddar S, Beaulieu L. Spectral method for the correction of the Cerenkov light effect in plastic scintillation detectors: A comparison study of calibration procedures and validation in Cerenkov light-dominated situations. Med Phys 2011;38:2140-50.
11. Carrasco P, Jornet N, Jordi O, Lizondo M, Latorre-Musoll A, Eudaldo T, *et al.* Characterization of the Exradin W1 scintillator for use in radiotherapy. Med Phys 2015;42:297-304.
12. Galavis PE, Hu L, Holmes S, Das IJ. Characterization of the plastic scintillation detector Exradin W2 for small field dosimetry. Med Phys 2019;46:2468-76.
13. Partanen M, Niemelä J, Ojala J, Keyriläinen J, Kapanen M. Properties of IBA Razor Nano Chamber in small-field radiation therapy using 6 MV FF, 6 MV FFF, and 10 MV FFF photon beams. Acta Oncol 2021;60:1419-24.
14. Planskoy B. Evluation of diamond radiation dosemeters. Phys Med Biol 1980;25:519-32.
15. Talamonti C, Kanxheri K, Pallotta S, Servoli L. Diamond detectors for radiotherapy X-ray small beam dosimetry. Front Phys 2021;9:632299. Available from: https://www.frontiersin.org/articles/10.3389/fphy.2021.632299/full. [Last accessed on 2022 Feb 10].
16. Rogers DW, Faddegon BA, Ding GX, Ma CM, We J, Mackie TR. BEAM: A Monte Carlo code to simulate radiotherapy treatment units. Med Phys 1995;22:503-24.
17. Kawrakow I. Accurate condensed history monte carlo simulation of electron transport. I. EGSnrc, the new EGS4 version. Med Phys 2000;27:485-98.
18. Low DA, Harms WB, Mutic S, Purdy JA. A technique for the quantitative evaluation of dose distributions. Med Phys 1998;25:656-61.
19. Reggiori G, Stravato A, Mancosu P, Lobefalo F, Paganini L, Zucconi F, *et al.* Small field characterization of a Nanochamber prototype under flattening filter free photon beams. Phys Med 2018;49:139-46.
20. Russo S, Reggiori G, Cagni E, Clemente S, Esposito M, Falco MD, *et al.* Small field output factors evaluation with a microDiamond detector over 30 Italian centers. Phys Med 2016;32:1644-50.
21. Ciancaglioni I, Marinelli M, Milani E, Prestopino G, Verona C, Verona-Rinati G, *et al.* Dosimetric characterization of a synthetic single crystal diamond detector in clinical radiation therapy small photon beams. Med Phys 2012;39:4493-501.
22. Monasor Denia P, Castellet García MD, Manjón García C, Quirós Higueras JD, de Marco Blancas N, Bonaque Alandí J, *et al.* Comparison of detector performance in small 6 MV and 6 MV FFF beams using a Versa HD accelerator. PLoS One 2019;14:e0213253.